

## **A semi-probabilistic GIS-based method for meso-scale flood hazard zonation**

R. De Risi<sup>1</sup>, F. Jalayer<sup>1,2</sup>, F. De Paola<sup>3</sup>, G. Manfredi<sup>1,2</sup>

<sup>1</sup>Department of Structures for Engineering and Architecture, University of Naples Federico II, Via Claudio 21, 80125 Napoli; email: raffaele.derisi@unina.it, fatemeh.jalayer@unina.it, gaetano.manfredi@unina.it

<sup>2</sup>Analysis and Monitoring of Environmental Risks (AMRA), Scarl, Naples, Italy.

<sup>3</sup>Department of Civil Architectural and Environmental Engineering, University of Naples Federico II, Via Claudio 21, 80125 Napoli; email: depaola@unina.it

### **ABSTRACT**

Identification of the flood-prone areas can be considered as a fundamental step in a flood risk management procedure. This work focuses on a fast procedure for hazard zoning within the flood-prone areas at a meso-scale. To this end, a semi-probabilistic GIS-based methodology for hazard zoning of the potentially flood-prone areas is presented. The main output consists of GIS-compatible maps for the hazard zoning (by flood height) of the potentially flood-prone areas. A flood height-dependent extension of the topographic wetness index (TWI) threshold is proposed as the lower-limit TWI for zones with flood height larger than a prescribed value. This procedure relies on calibrating the flood height-dependent topographic wetness index (TWI) threshold through maximum likelihood estimation and based on the inundation profiles calculated at micro-scale level for a given spatial window. This calibration is performed for different values of flood depth in order to investigate the correlation between the TWI threshold and the flood depth conditioned on return period, through simple linear regression. The resulting regression model is used in order to up-scale the results from the micro-scale spatial window to the meso-scale level. As a demonstration, the procedure has been applied for the city of Addis Ababa, Ethiopia.

### **INTRODUCTION**

Delineation of flood-prone areas and evaluation of the exposure to risk in the urban areas are fundamental steps in taking adaptive measures for flood risk mitigation. Flood hazard zoning can be particularly useful for obtaining preliminary flood risk maps on a meso-scale. Clearly, these maps can be used for a fast screening of critical areas and cannot replace accurate hydraulic calculations. The flood-prone areas are usually identified based on available historical flooding data or by defining a buffer zone around the rivers (see [Gall et al. 2007](#) or [Apel et al. 2009](#) for a comprehensive discussion on identification of flood prone areas). A recent work by [Degiorgis et al. 2012](#) employs pattern classification techniques for the delineation of flood-prone areas and hazard graduation within these areas based on remote-sensed data.

This work presents a semi-probabilistic GIS-based methodology for hazard zoning of potentially flood-prone areas. The output of this work is presented as GIS-compatible maps of hazard zonation (by flood height) of the potentially flood prone urban areas at the meso-scale level. Upon necessary field verifications, these maps can be used as supplementary technical support for flood risk mitigation and emergency preparedness.

In a previous work (Jalayer et al. 2013), the authors demonstrate how the potentially flood-prone areas (i.e. areas identified as those with a topographic wetness index greater than a specific threshold) can be delineated through a Maximum likelihood estimation procedure applied to a spatial window in micro-scale. In this work, the concept of potentially flood-prone areas is extended in order to define a flood depth-dependent TWI threshold. Such a threshold marks the lower-bound TWI for areas with flood depth larger than a prescribed depth value given the return period. Maximum likelihood parameter estimation is then applied in order to obtain a probability distribution for the TWI threshold that corresponds to a prescribed flood depth and return period. This procedure, performed for different levels of flood depth, will help in characterizing the correlation between TWI threshold and flood depth, conditioned on a given return period. Up-scaling the results obtained for the spatial window at the micro scale level to the meso-scale, potentially flood-prone areas distinguished by flood depth larger than a specific value and conditioned on the return period can be delineated.

The proposed procedure has been applied to the city of Addis Ababa, Ethiopia. In particular the maximum likelihood calibration of the TWI threshold for different values of flood depth has been performed on the area of Little Akaky, in the south of the city. The up-scaled hazard zoning of the flood-prone areas will be compared with the flood profiles calculated through the hydraulic routine for another zone in the city.

## METHODOLOGY

**Delineation of flood-prone areas using the TWI.** The topographic wetness index (Kirkby 1975, Quin et al. 2011) has been shown to be strongly correlated to the area exposed to flood inundation (Manfreda et al. 2007; 2008; 2011). The TWI allows for the delineation of a portion of a hydrographic basin potentially exposed to flood inundation (referred to herein as flood prone or more briefly as FP), by identifying all the areas characterized by a topographic index that exceeds a given threshold. The TWI threshold value depends on the resolution of the digital elevation model (DEM), the geomorphology of the hydrographic basin, and the presence of constructed infrastructures (such as, sewage system, bridges and culverts, etc.). This threshold is usually calibrated based on the results of detailed delineation of the inundation profile for selected zones (Jalayer et al. 2013). The inundation profile, reported as the flood depths (and velocities) for various nodes within a lattice covering a given area for different return periods, can be obtained by means of classic hydraulic routines of various degrees of sophistication and accuracy (Apel et al. 2009). The TWI threshold can also be calibrated based on available spatial extent of previous flooding events (De Risi et al. 2013).

### Definition of the flood-depth dependent TWI threshold

The flood depth dependent TWI threshold can be defined as the TWI value that marks the lower-bound value for the zones with flood depth larger than a prescribed value, conditioned on a given return period. Herein, the flood profile calculated for a given spatial window in micro-scale is used in order to evaluate the flood depth-dependent TWI thresholds, for a given return period.

**Maximum likelihood estimation of TWI threshold.** Let  $W$  represent a designated spatial window (within the basin), for which, the inundation profile is calculated. Moreover, let  $FP$  represent the flood-prone areas (identified as  $TWI > \tau(h(T_R))$ ) (for brevity, we refer to it as  $\tau$ ). Let  $IN(T_R)$  represent the inundated areas for a given return period  $T_R$  identified as  $h > h(T_R)$ .  $h(T_R)$  is flood depth calculated for a given point within the zone of interest  $W$ . Figure 1(a) illustrates, in a schematic manner, spatial window  $W$  and the extents identified as  $FP$  and  $IN(T_R)$ .

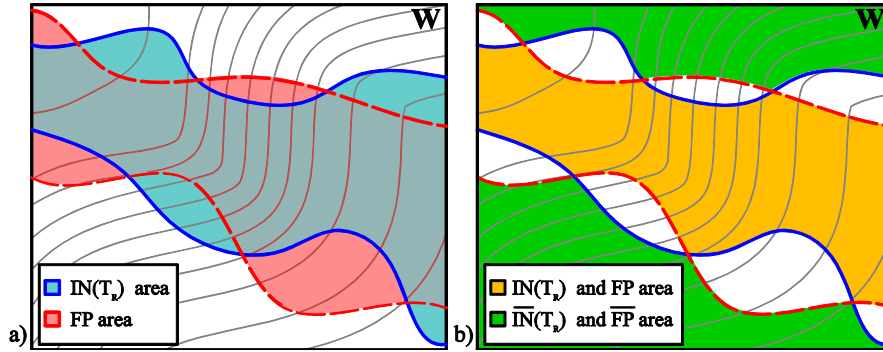


Figure 1. FP and IN areas

The probability of the correct delineation of the flood-prone areas or the likelihood function for the TWI threshold  $\tau$  denoted as  $L(\tau|W)$  for various values of  $\tau$  can be calculated as following:

$$L(\tau|W) = P(FP, IN(T_R) | \tau, W) + P(\overline{FP}, \overline{IN(T_R)} | \tau, W) \quad (1)$$

where  $P(FP, IN(T_R) | \tau, W)$  denotes the probability that a given point within zone  $W$  is identified both as flood-prone  $FP$  (using the TWI method) and inundated  $IN(T_R)$  (using the more accurate inundation profiles), for a given return period  $T_R$  and conditioned on (the  $|$  sign) a given value of  $\tau$  of the TWI threshold. The area identified as both  $FP$  and  $IN(T_R)$  is indicated by color orange in Figure 1(b). Similarly,  $P(\overline{FP}, \overline{IN(T_R)} | \tau, W)$  denotes the probability that a given point within the zone of interest is neither identified as  $FP$  nor as  $IN(T_R)$ , conditioned on a given value of  $\tau$  of the TWI threshold. The area identified as not  $FP$  and not  $IN(T_R)$  is indicated by color green in Figure 1(b).

In the Eq. 1, the terms  $P(FP, IN | \tau, W)$  and  $P(\overline{FP}, \overline{IN} | \tau, W)$  can be expanded, using the probability theory's product rule (Jaynes, 1995), as following:

$$P(FP, IN(T_R) | \tau, W) = P(FP | \tau, W) \cdot P(IN(T_R) | FP, \tau, W) \quad (2)$$

$$P(\overline{FP}, \overline{IN(T_R)} | \tau, W) = P(\overline{FP} | \tau, W) \cdot P(\overline{IN(T_R)} | \overline{FP}, \tau, W) \quad (3)$$

where the term  $P(IN(T_R)|FP, \tau, W)$  denotes the probability of being  $IN(T_R)$  given that it is identified as  $FP$  and  $P(\overline{IN(T_R)}|\overline{FP}, \tau, W)$  denotes the probability of not being  $IN(T_R)$  conditioned on not being  $FP$ , given the threshold value  $\tau$ . The terms  $P(FP|\tau, W)$  and  $P(\overline{FP}|\tau, W)$  represent the probability of being  $FP$  or not being  $FP$ , respectively, given the TWI threshold value  $\tau$ .

### Estimation of the likelihood function using the areal extents.

**Part 1 - The micro-scale estimations.** Let  $A_W(FP)$  denote the areal extent of the flood prone portion of the zone  $W$  identified via the TWI method (i.e., the extent of the portion colored as red in Figure 1(a)).  $A_W(IN(T_R))$  is the areal extent of the inundated portion of  $W$ , identified via hydraulic calculations, for a given return period (i.e., the extent of the portion colored as blue in Figure 1(a)). Analogously,  $A_W(\overline{FP})$  and  $A_W(\overline{IN(T_R)})$  refer to the areas of the not flood prone and not inundated portions, respectively. The probability terms  $P(IN(T_R)|FP, \tau, W)$  and  $P(\overline{IN(T_R)}|\overline{FP}, \tau, W)$  can be estimated by the ratio of areal extents, as expressed in the following:

$$P(IN(T_R)|FP, \tau, W) = \frac{A_W(IN(T_R), FP)}{A_W(FP)} \quad (4)$$

$$P(\overline{IN(T_R)}|\overline{FP}, \tau, W) = \frac{A_W(\overline{IN(T_R)}, \overline{FP})}{A_W(\overline{FP})} \quad (5)$$

where  $A_W(IN(T_R), FP)$  denotes the areal extent of the portion of the area  $W$  that is both  $FP$  and  $IN(T_R)$  (i.e., the extent of the area colored as orange in Figure 1(b));  $A_W(\overline{IN(T_R)}, \overline{FP})$  denotes the areal extent of the portion of the area  $W$  that is neither  $FP$  nor  $IN(T_R)$  (i.e., the extent of the area colored as green in Figure 1(b)). As mentioned above, the areal extents  $A_W(IN(T_R), FP)$ ,  $A_W(\overline{IN(T_R)}, \overline{FP})$ ,  $A_W(FP)$  and  $A_W(\overline{FP})$  are all functions of the TWI threshold  $\tau$ .

**Part 2 - The meso-scale estimations.** In the previous section, it was demonstrated how  $P(IN(T_R)|FP, \tau, W)$  and  $P(\overline{IN(T_R)}|\overline{FP}, \tau, W)$  were estimated using the areal extent ratios, that were calculated in a micro-scale delineated by window  $W$ . However, also  $P(FP|\tau, W)$  and  $P(\overline{FP}|\tau, W)$  need to be estimated in order to be able to calculate the likelihood function in Eq. 1. It has been chosen to estimate the above two terms using the areal extents calculated in the meso-scale (city-scale). Denoting the total administrative area of the city under consideration as  $A_{urban}$  and denoting the total areal extent within the city having TWI greater than the given threshold  $\tau$  as  $A_{urban}(FP)$ , one can estimate the term  $P(FP|\tau)$  as:

$$P(FP|\tau) = \frac{A_{urban}(FP)}{A_{urban}} \quad (6)$$

The probability  $P(\overline{FP}|\tau)$  can then be calculated as  $1 - P(FP|\tau)$ .

Finally, the likelihood function in Eq. 1 can be calculated by substituting the terms calculated in Equations 4, 5, and 6 in Eqs. 2 and 3, and summing up these two last equations. The maximum likelihood estimate for the TWI threshold can then be calculated as the  $\tau$  value that maximizes the likelihood function in Eq. 1.

**Correlation between flood depth and TWI.** The maximum likelihood estimation of the flood depth-dependent TWI threshold is performed for various prescribed flood depth values, conditioned on a given return period. Herein, a simple linear regression model is used in order to probabilistically characterize the correlation between TWI threshold and the flood depth. In such a model, the conditional expected value for flood depth corresponding to a given value of TWI threshold  $\tau$  and conditioned on a return period value equal to  $T_R$  can be calculated as.

$$E[h(T_R)|\tau] = a(T_R) \cdot \tau + b(T_R) \quad (7)$$

The conditional standard deviation for flood depth given TWI threshold can be estimates as the standard error of regression:

$$\sigma[h(T_R)|\tau] = \sqrt{\sum_i (h_i(T_R) - a(T_R) \cdot \tau_i - b(T_R))^2 / (n-2)} \quad (8)$$

where  $i=1:n$ , and  $n$  is the number of  $h(T_R)$  and  $\tau$  pairs used in the regression.

## CASE STUDY

The methodology described herein is implemented in order to perform hazard zoning of the flood prone areas in the city of Addis Ababa, (for brevity referred to also as Addis), Ethiopia (Figure 2a). The city is situated in the high plateau of central Ethiopia in the North-South oriented mountain systems neighboring the Rift-Valley. The city is overlooked by Mount Yarer in the east, Mount Entoto in the north and Mount Wochecha in the west. Several small streams originate in the mountains surrounding the city and flow into the metropolitan area of Addis Ababa. Torrential rains, which are common during the rainy season, cause a sudden rise in the flow of these streams and periodically inundate the settlements built along their banks. The flooding of August 2006 was the worst in the Ethiopian history. It affected 363000 people and left approximately 200000 people homeless. The final death toll was estimated at around 647 but the impacts on health and well-being were much larger. Lifelines were affected across the whole country. For instance, the telephone and power lines were interrupted and the main roads to Addis Ababa were blocked, rendering the city inaccessible. Last but not least, the floods had a severe impact on urban agriculture, leading to widespread food shortages in one of the world's poorest states. The topographic wetness index is calculated in a GIS framework based on a digital elevation model of the city (Year: 2007, vertical resolution: 1 meters). Figure 2b illustrates the resulting TWI map for Addis. It can be observed that the TWI

values vary between 7 and 22.78. In particular, largest TWI values can be spotted around the natural water channels.

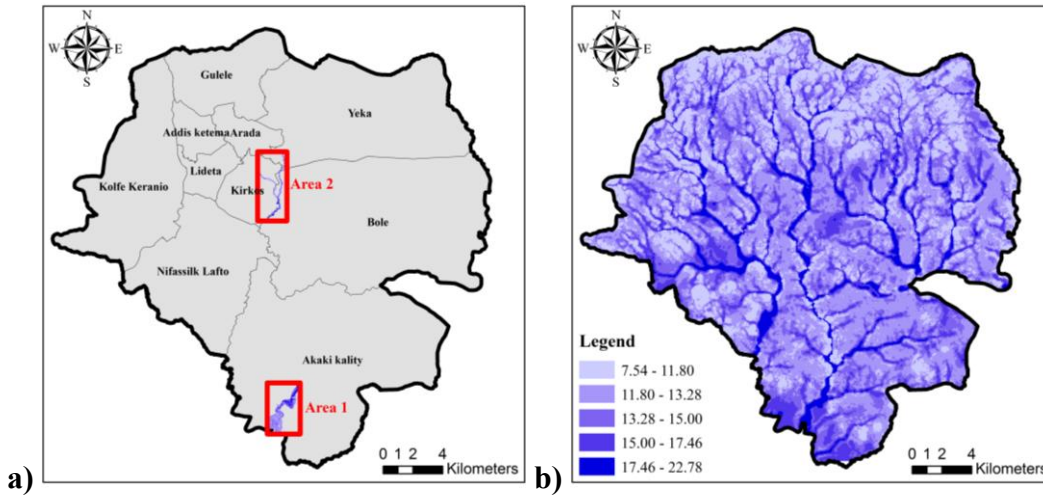


Figure 2. a) the city of Addis Ababa, b) the TWI map

In order to calibrate the TWI threshold for Addis, the inundation profile for various return periods have been calculated for the Little Akaki area (Area 1, Figure 2a), located in the southern part of Addis. Little Akaki is known to be a flood-prone area, based on past flooding experiences. The inundation profile has been calculated by two-dimensional simulation of flood volume propagation using the software FLO2D (O'Brien et al., 1993; FLO-2D, 2004) (using historical rainfall records, the DEM, and the calculation of the hydrograph based on the SCS Curve Number method (SCS, 1972)) assuming a simulation time of 45 hours. The outcome of the hydraulic analyses are calculated for six return periods ( $T_R = 2, 10, 30, 50, 100$  and  $300$  years). The flood depths for a return period of  $T_R = 300$  yrs calculated for Area 1 are plotted in Figure 3a. Moreover, for the purpose of verification, the hydraulic profile has also been calculated for the Area 2 (Figure 2a), located between Arada, Yeka, Bole and Kirkos sub-cities, in the central part of Addis. The flood depth values for Area 2 corresponding to  $T_R = 300$  yrs are plotted in Figure 3b.

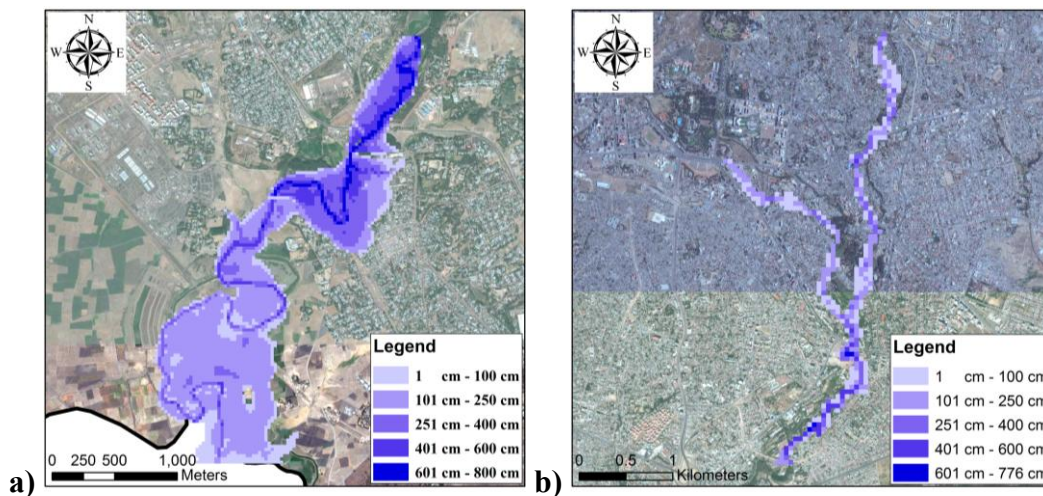


Figure 3. Inundation profiles corresponding to  $T_R = 300$  years for a) Area1, and b) Area2

**Maximum likelihood estimation of flood-prone threshold.** The resulting likelihood function  $L(\tau|W)$  for a return period of  $T_R=100$  years and for a flood depth larger than  $h(T_R)=0$ , is plotted in Figure 4 as a function of the TWI threshold  $\tau$ . Consequently, the maximum likelihood estimate for  $\tau$  (i.e., the value that corresponds to the maximum likelihood) can be identified as  $\tau=17.11$ . Furthermore, by identifying the  $\tau$  values corresponding to more than 99% of the maximum likelihood value, it is possible to define a maximum likelihood interval, that varies between  $\tau_{ML}^- = 16.66$  and  $\tau_{ML}^+ = 17.89$ . That is, from a practical point of view, the information used for calibrating the TWI threshold leads to identifying a maximum likelihood interval [16.66, 17.89] for  $\tau$ .

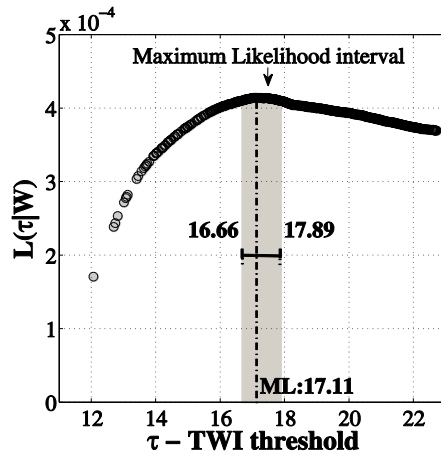


Figure 4. The likelihood function for TWI threshold  $\tau$  for flood depth values larger than  $h(T_R)=0$

Applying the same procedure for flood depth values larger than  $h(T_R)=h$ , the maximum likelihood estimates for TWI threshold  $\tau$  can be obtained, conditioned on a prescribed return period  $T_R$ . Figure 5 illustrates the linear regression of  $h(T_R)$  versus corresponding maximum likelihood  $\tau$  estimates, for various return periods  $T_R$ . It can be observed, that in most cases, the data pairs are contained within the mean plus/minus one standard deviation interval.

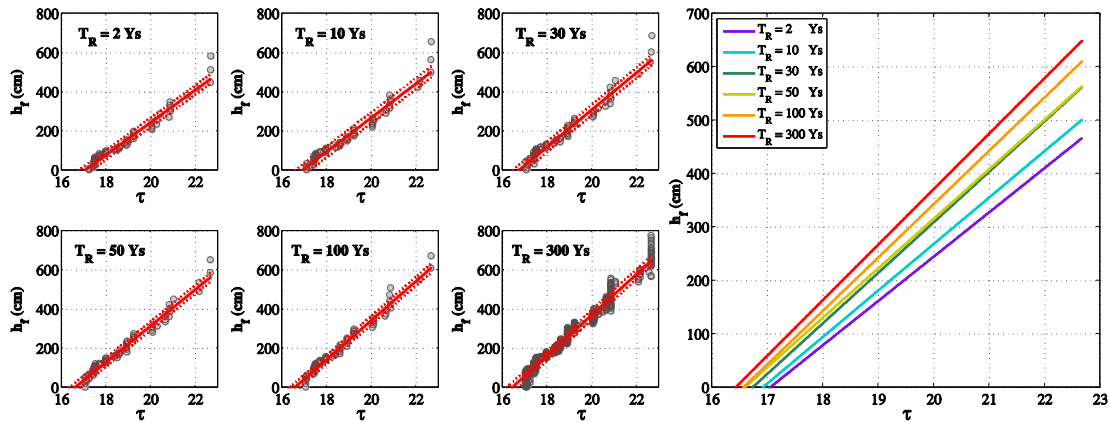
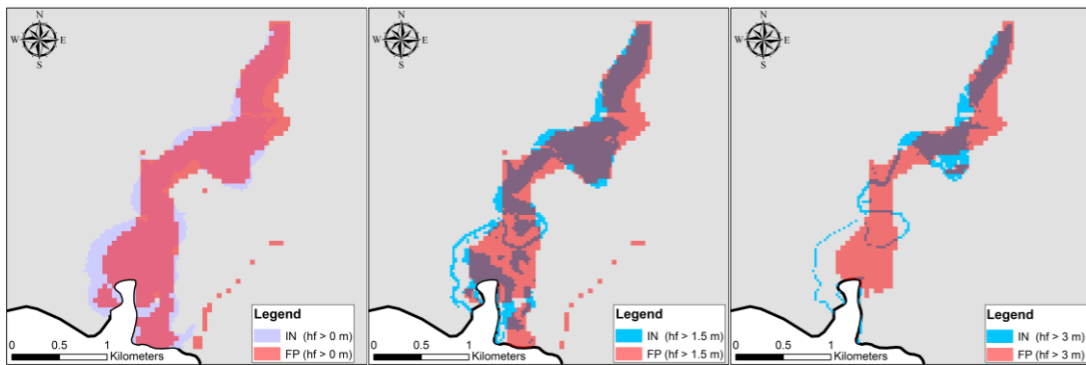


Figure 5. The linear regression of  $h(T_R)$  versus corresponding maximum likelihood  $\tau$  estimates, for various return periods  $T_R$ .

It can be observed, from the regression prediction lines plotted as a function of return period in the right-hand column of Figure 5, that the correlation between  $h(T_R)$

and  $\tau$  is sensitive to the prescribed return period. These regression predictions can be used for up-scaling the results to the meso-scale level. That is, for a given return period, the TWI values can be substituted with the corresponding regression prediction for  $h(T_R)$ .

**Overlay of the hydraulic routine results (IN) and flood prone areas zonation (FP).** A visual check of the accuracy of the results can be performed by overlaying the inundated zones (obtained from the hydraulic routine) and the TWI map for threshold values larger than the maximum likelihood estimate  $\tau_{ML}$ , calculated for different values of flood depth and for  $T_R=300$  Ys. Fig. 6 below illustrates the result of overlaying the hydraulic profile and  $TWI > \tau_{ML}$  corresponding to  $T_R$  equal to 300, for the Area 1 and for the three flood depth values  $h(T_R)=0.0, 1.5$  and  $3.0$  m.



**Figure 6. Area 1: Overlay of the hydraulic routine results (IN) and flood prone areas zonation (FP) for three values of flood depth (0, 1.5 and 3 m)**

The hydraulic profile (IN) for Area 2 has also been overlaid with the flood prone areas zonation (FP) for various flood depth values  $h(T_R)=0.0, 1.5$  and  $3.0$  m, conditioned on  $T_R=300$  yrs. It should be noted that, in contrast to the hydraulic profile for Area 1 that has been used for calibrating the flood depth-dependent TWI values, the hydraulic results for Area 2 has not been used for calibrating the TWI threshold.

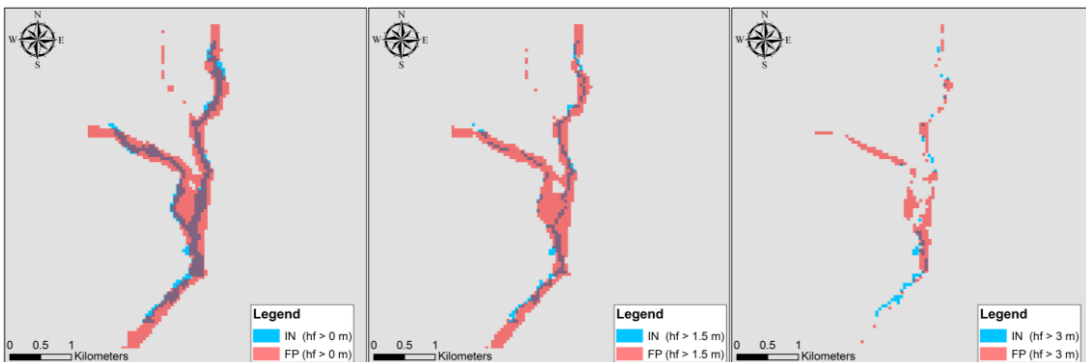


**Figure 7. Area 2: Overlay of the hydraulic routine results (IN) and flood prone areas zonation (FP) for three values of flood depth (0, 1.5 and 3 m)**

Observing Figures 6 and Figure 7, one can observe a fair agreement between the inundated areas (based on the hydraulic routine) and the flood prone areas zonation, and not only for the spatial window in which the procedure was calibrated.



## UPSCALING

The regression model developed previously can be used in order to upscale the results to the meso-scale. This can be done by first defining the flood depth thresholds that mark the hazard zonation boundaries. Figure 8 below shows the meso-scale hazard map for return periods of 30 and 300 years in which the hazard zonation thresholds are defined as follows: 0.0 – 1.0 m, 1.0 – 3.0 m, and larger than 3.0 m.

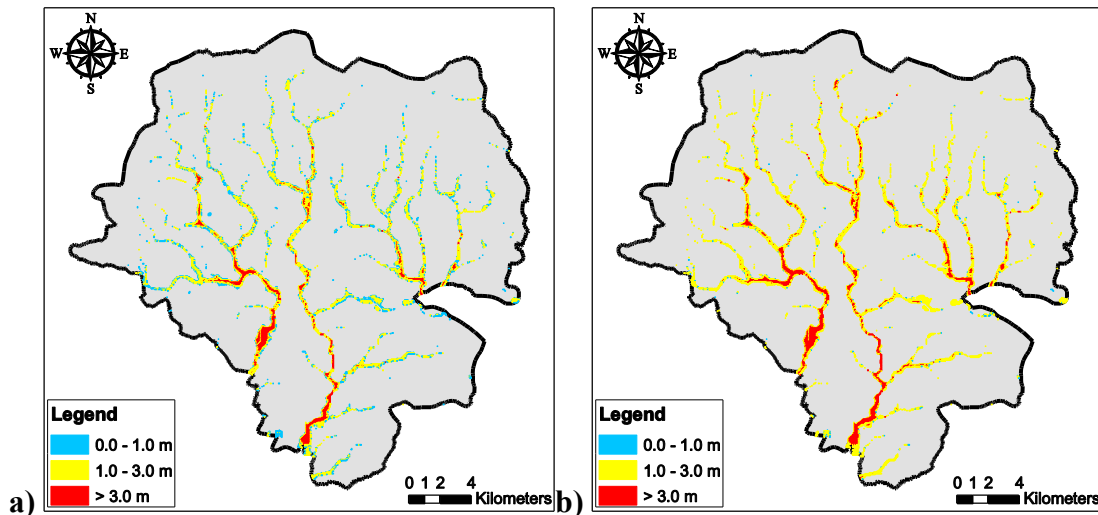


Figure 8. Meso-scale flood hazard maps for a)  $T_R=30$  Ys and b)  $T_R=300$  Ys

## CONCLUSION

A GIS-based semi-probabilistic method is presented for the zonation of flood prone areas. This work extends the definition of flood prone areas (areas characterized as having flood depth values larger than zero), as those with a topographic wetness index (TWI) larger than a certain threshold, by defining flood depth-dependent TWI threshold for various depths and conditioned on a prescribed return period. For a given flood depth value, maximum-likelihood estimate for the TWI threshold is obtained by maximizing the probability of a correct identification of the contour with flood depth values larger than the specified value, conditioned on the return period and for a spatial window in micro scale. The resulting TWI threshold versus flood depth pairs are used inside a linear regression scheme in order to create a predictive model for flooding depth as a function of the TWI threshold and given the return period. The predictive regression model is verified visually for another spatial window (outside the zone where the model has been calibrated). Finally, this model is used for up-scaling the results into meso-scale. These leads to hazard zonation maps for various return periods. Such maps, in absence of more accurate results, can be used for a rapid screening and identification of areas that need immediate actions and more detailed evaluations.

## ACKNOWLEDGEMENTS

This work was supported in part by the European Commission's seventh framework program Climate Change and Urban Vulnerability in Africa (CLUVA), FP7-ENV-2010, Grant No. 265137. This support is gratefully acknowledged.

## REFERENCES

- Apel, H., Aronica, G.T., Kreibich, H., Thielen, A.H. (2009). "Flood risk analyses—how detailed do we need to be?". *Nat. Hazard*, 49:79–98.
- Degiorgis M., Gnecco G., Gorni S., Roth G., Sanguineti M., and Taramasso A.C., Classifiers for the detection of flood-prone areas using remote sensed elevation data. *Journal of Hydrology*, 2012. 470-471: p. 302-315.
- De Risi, R., Jalayer, F., De Paola, F., Giugni, M. (2013). Probabilistic GIS-based Delineation of Flood-prone areas based on Digital Elevation Model and Historical Flooding Extent: The case of Ouagadougou, special issue on *Boletín Geológico y Minero* (under review).
- FLO-2D Software, Inc, 2004. FLO-2D® User's Manual, Nutrioso, Arizona, [www.flo-2.com](http://www.flo-2.com).
- Gall, M., Boruff, B. J., & Cutter, S. L. (2007). Assessing flood hazard zones in the absence of digital floodplain maps: comparison of alternative approaches. *Natural Hazards Review*, 8(1), 1-12.
- Jalayer F., De Risi, R., De Paola, F., Giugni, M., Manfredi, G., Gasparini, P., Topa, M.E., Yonas, N., Yeshitela, K., Nebebe, A., Cavan, G., Lindley, S., Printz, A., Renner, F. (2013) Probabilistic GIS-based method for delineation of flood-prone areas and identification of urban hotspots. Under review in *Natural Hazards*.
- Jaynes, E.T. (1995). "Probability Theory: The logic of science". Book.
- Kirkby, M. J. (1975). "Hydrograph modelling strategies". *Progress in physical and human geography*, R. F. Peel, M. D. Chisholm, and P. Haggett, eds., Heinemann, London, 69-90.
- Manfreda, S., Sole, A., and Fiorentino, M. (2007). "Valutazione del pericolo di allagamento sul territorio nazionale mediante un approccio di tipo geomorfologico." *L'Acqua*, 4, 43-54 (in Italian).
- Manfreda, S., Sole, A., and Fiorentino, M. (2008). "Can the basin morphology alone provide an insight on floodplain delineation?" *On flood recovery innovation and response*, WIT, Southampton, UK, 47-56.
- Manfreda, S., Di Leo, M., Sole, A. (2011). "Detection of Flood-Prone Areas Using Digital Elevation Models." *Journal of Hydrologic Engineering*, Vol. 16, No. 10, ASCE, 781-790
- O'Brien JS, Julien PY, and Fullerton WT (1993) Two-dimensional water flood and mudflow simulation. *Journal of Hydraulic Engineering* 119 (2): 244-261.
- Qin, Z.c., Zhu, A.X., Pei, T., Li, B.L., Scholten, T., Behrens, T., Zhou, C.H. (2011). "An approach to computing topographic wetness index based on maximum downslope gradient". *Precision Agric*, 12:32–43.